Form and function of F-actin during biomineralization revealed from live experiments on foraminifera

Jarosław Tyszka[a,1], Ulf Bickmeyer[b], Markus Raitzsch[c,d], Jelle Bijma[c], Karina Kaczmarek[c], Antje Mewes[c], Paweł Topa[e], and Max Janse[f]

[a]Research Centre in Kraków, Institute of Geological Sciences, Polish Academy of Sciences, 31-002 Kraków, Poland; [b]Ecological Chemistry, Alfred-Wegener-Institut Helmholtz-Zentrum für Polar- und Meeresforschung, D-27570 Bremerhaven, Germany; [c]Marine Biogeosciences, Alfred-Wegener-Institut Helmholtz-Zentrum für Polar- und Meeresforschung, D-27570 Bremerhaven, Germany; [d]Institut für Mineralogie, Leibniz Universität Hannover, 30167 Hannover, Germany; [e]Department of Computer Science, AGH University of Science and Technology, 30-052, Kraków, Poland; and [f]Burgers' Ocean, Royal Burgers' Zoo, 6816 SH Arnhem, The Netherlands

Edited by Lia Addadi, Weizmann Institute of Science, Rehovot, Israel, and approved January 23, 2019 (received for review June 15, 2018)

Although the emergence of complex biomineralized forms has been investigated for over a century, still little is known on how single cells control morphology of skeletal structures, such as frustules, shells, spicules, or scales. We have run experiments on the shell formation in foraminifera, unicellular, mainly marine organisms that can build shells by successive additions of chambers. We used live imaging to discover that all stages of chamber/shell formation are controlled by dedicated actin-driven pseudopodial structures. Successive reorganization of an F-actin meshwork, associated with microtubular structures, is actively involved in formation of protective envelope, followed by dynamic scaffolding of chamber morphology. Then lamellar dynamic templates create a confined space and control mineralization separated from seawater. These observations exclude extracellular calcification assumed in selected foraminiferal clades, and instead suggest a semiintracellular biomineralization pattern known from other unicellular calcifying and silicifying organisms. These results give a challenging prospect to decipher the vital effect on geochemical proxies applied to paleoceanographic reconstructions. They have further implications for understanding multiscale complexity of biomineralization and show a prospect for material science applications.

morphogenesis | biomineralization | shells | foraminifera | cytoskeleton

Single cells are capable of constructing a wide range of sophisticated organic/inorganic composite structures used for mechanical support, defense, photodamage protection, acceleration of photosynthesis, and cell compartmentalization (1, 2). Eukaryotic cells share fundamental and universal morphogenetic mechanisms already studied by D'Arcy Thomson over a century ago (3). Although we are aware that these mechanisms are expressed by self-assembling proteins and their supramolecular structures (4, 5), intracellular interactions responsible for shell growth and form in single cells are still highly unclear. We have chosen foraminifera that build elaborate and diverse shells (tests) to investigate cellular mechanisms responsible for morphogenesis and biomineralization.

Foraminifera are unicellular eukaryotes, characterized by anastomosing granular pseudopodial networks called granuloreticulopodia (6–9). Most foraminifera construct shells (tests), using diverse materials, in several different ways from synthesis of organic compounds, through agglutination of sediment grains, to secretion of calcium carbonate (1, 10) (Fig. 1 and *SI Appendix*, Figs. S1–S3). These shells are known from a long and nearly continuous fossil record. Foraminifera constructing calcareous shells belong to one of the main carbonate producers in the oceans with almost 25% of the global oceanic $CaCO_3$ production (11). For over the last 500 Mya, foraminifera have evolved an extreme morphologic and textural diversity of shells (1) providing an archive of past climate and evolution (10, 12). Two main classes (Globothalamea and Tubothalamea) identified on the basis of small subunit rDNA records have developed distinct morphogenetic strategies (13). Their shell morphogenesis can be understood in terms of chamber-by-chamber formation (1, 14).

Pioneers who studied living foraminifera described that chamber formation was progressing on what they called "active matrix" (15, 16). Hottinger (1) suggested that foraminiferal chamber morphology depended on the length of rhizopodia (branching pseudopodia) extruded from the previous chamber and supported by microtubular cytoskeleton. Recent investigations on theoretical models of foraminiferal morphogenesis implied that the cytoskeleton, dominated by microtubular dynamics, is mainly responsible for shaping chambers (14, 17). Although actin role in chamber morphogenesis was also proposed and introduced to the preliminary model of actin meshwork–plasma membrane interactions (18), the lack of empirical studies has prevented any further progress in understanding a morphogenetic system in foraminifera.

The only knowledge on cytoskeletal association with biomineralization comes from silicifying or calcifying algae, represented by diatoms and haptophytes. Observations of fixed diatoms indicated a close association of labeled cytoskeletal structures with the SiO_2 frustule formation (19, 20). Further, actin inhibition experiments on coccolithophores showed either abnormal development (21) or a complete cessation of scales (22), known as coccoliths, and indicated that "actin plays an important role in biomineralization" (22). Such experiments have been limited to

Significance

Unicellular organisms form endless variability of complex skeletons that serve as archives of Earth's history and play a crucial role in global geochemical cycles. A longstanding question is how single cells control morphogenesis and mineralization of skeletal structures. Although already addressed by Sir D'Arcy W. Thompson, this problem is still unsolved. Shell emerges from a controlled cascade of interactions at different levels of cellular organization. To gain insight into its morphogenesis, we apply live fluorescent imaging to observe cytoskeleton structures during shell formation in foraminifera. Our live experiments on calcifying foraminiferal chambers show that dynamic F-actin structures are involved in shaping and controlling mineralization.

Author contributions: J.T. designed research; J.T. and M.R. performed research; U.B., J.B., K.K., A.M., P.T., and M.J. contributed new reagents/analytic tools; J.T. and M.R. analyzed data; K.K. and A.M. cultured foraminifera; P.T. cooperated in development of conceptual model tested in vivo; M.J. provided access to living foraminifera; and J.T., M.R., and J.B. wrote the paper.

The authors declare no conflict of interest.

This article is a PNAS Direct Submission.

[1]To whom correspondence should be addressed. Email: ndtyszka@cyfronet.pl.

This article contains supporting information online at www.pnas.org/lookup/suppl/doi:10.1073/pnas.1810394116/-/DCSupplemental.

Published online February 19, 2019.

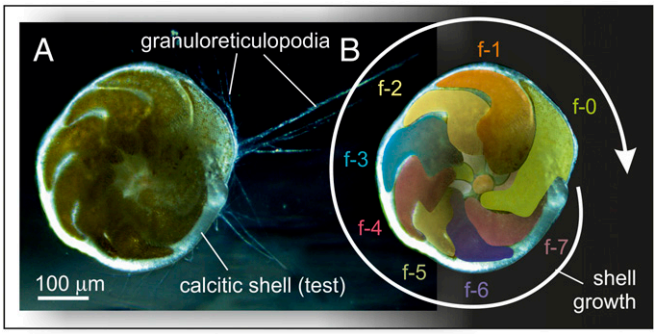

Fig. 1. Dorsal view of a living benthic foraminifera *A. lessonii*. (*A*) A specimen with extended granuloreticulopodia observed under the stereomicroscope. (*B*) The spiral (low helical) shell growths chamber by chamber and records ontogenesis. Eight youngest chambers in the final whorl are labeled from f-7 to f-0. An older internal whorl is nearly completely overlapped by the youngest chambers.

observations of either selected stages of biomineralization (19, 20) or final secretion inhibition, defects, and malformations (21, 22).

Recent progress in live actin staining (23) facilitates direct monitoring of actin dynamics in real time. The main objective of this study is to prove that actin is truly involved in morphogenesis of foraminiferal shells. We focus on spatial organization and dynamics of actin structural components and identification of their potential role in controlling shape and biomineralization. All observations are based on live experiments to recognize a complete, undisturbed succession of growth and mineralization stages.

Results

Active Role of Actin in Dynamic Scaffolding. We applied F-actin labeling to living foraminifera to identify actin cytoskeleton structures and their dynamics during morphogenesis and biomineralization of the shell. Experiments were carried out on *Amphistegina lessonii* d'Orbigny (Figs. 1–3), which belongs to Globothalamea (13), the most widespread foraminiferal group. This species secretes a perforate calcitic wall (Figs. 1*A* and 3*A*), which is formed on both sides [bilamellar calcification (14, 24)] of an organic matrix called the "primary organic sheet" (POS), interpreted as a template for $CaCO_3$ nucleation (15, 25–27).

Live SiR actin labeling shows a dynamic pattern of stained actin meshwork during the whole process of chamber formation recorded by time-lapse imaging (Fig. 2 and Movies S1–S6). At the onset of chamber formation, regular reticulopodial activity (Fig. 1*A*) is nearly ceased and finger-like protuberances are extended from the aperture (shell opening) and get attached to the substratum (glass surface) where they form an outer protective envelope (OPE) (15) (Figs. 2 *A* and *B*, 3*C*, and 4*B* and Movie S1). The OPE in its early, i.e., dynamic, stage is labeled with SiR-actin (marked in red on Fig. 2*A*), showing actin meshwork activity associated with a membranous surface of the structure. After ∼100 min, a globular bulge (globopodium) appears from the same aperture inside the OPE and is then continuously extended to form the chamber morphology (Fig. 2 *B* and *C* and Movie S2). This dynamic globular bulge is herein called globopodium to differentiate from other modes of pseudopodial organizations. After 2.5–3.5 h from the onset of chamber formation (Fig. 2*C*), the globopodium is remodeled to the stage of dense "radiating rhizopodia" (28) with a spongy microstructure strongly labeled by the actin dye. An aperture, as an opening in the globopodium, is also formed at this stage of chamber formation (Fig. 2*C* and Movie S3). At the same time, the actin meshwork is gradually withdrawn from the OPE (Fig. 2 *C*–*F*). As a consequence, in the later stage of chamber formation, the OPE remains immobile (static) and attached to the substratum (bottom glass of the Petri dish). From now on, OPE is inactive and moves passively, following movement of the whole individual. The globopodial stage of chamber formation (Fig. 2 *B*–*D*) takes between 1 and 2 h and finishes with the consolidation of the chamber shape (Fig. 2*D* and Movie S4) and the start of biomineralization (Fig. 2*E* and Movie S5). The onset of biomineralization apparently starts after the stabilization of the final chamber morphology (Fig. 2*D*) and before the appearance of pores that penetrate the shell wall (Fig. 2*E*). This is associated with reorganization of dense radiating rhizopodia into sparsely distributed, frothy pseudopodia. Fig. 2 *D*–*F* shows such a transition from the globopodium supported by a dense actin meshwork infilling the whole chamber volume to a frothy pseudopodium that forms a delicate pseudopodial sponge-like structure with nearly invisible actin meshworks. This three-dimensional structure penetrates an internal part of a chamber and appears to be in direct contact with seawater via its aperture (Fig. 4 *A* and *D*). It connects the site of chamber formation and the cell body and probably facilitates cell signaling and transport of cytoplasmic components, as well as inorganic substrates required for biomineralization.

We further ran supplementary live experiments applying double labeling based on calcein acetoxymethyl ester (Calcein AM) and SiR-actin. This cell-permeant dye hydrolyzed to calcein intracellularly and was used to identify morphology and dynamics of active cytoplasmic structures (29) involved in chamber formation. Calcein itself is a Ca^{2+} and Mg^{2+} fluorescent indicator that is applied to stain biogenic calcium carbonates/phosphates precipitated in bones, skeletons, and shells, including foraminiferal tests (30). In contrast to the nonpermeable calcein (30), Calcein AM, a nonfluorescent acetomethoxy derivate of calcein, neither stains seawater nor the calcified shell (29).

The double-staining experiments were relatively short (up to 20 min) due to phototoxicity of two lasers simultaneously used for the confocal microscopy. Longer exposure to both lasers interrupted chamber formation and caused withdrawal of the cytoplasm. Staining results show (Fig. 3 *C*–*E* and *SI Appendix*, Figs. S4 and S5) a close match of Calcein AM and SiR-actin fluorescent signals associated with chamber formation. Calcein AM marks globopodial structures formed by a dense 3D rhizopodial network filled with a fine internal actin meshwork (Fig. 3 *D* and *E*). Calcein staining follows the same spongy pattern identified by the actin dye. These results indicate that the globopodium is not completely filled with dense cytoplasm, but instead, forms a spongy pseudopodial network supported by 3D actin meshworks (Fig. 3*C*). This dynamic microstructure is gradually transformed to a frothy pattern identified during biomineralization of the chamber wall (Fig. 2).

All transmitted and fluorescent light observations of active pseudopodial structures show bidirectional movement of granules that follow relatively straight and often anastomosing tracks (Movies S1–S6). Such motility is limited to cytoplasmic structures stained by Calcein AM and associated with SiR-actin staining. This movement is not observed within static structures, such as the OPE at its nonmotile stage (Fig. 2). The active stage of the OPE presents vigorous bidirectional streaming along all its reticulate branches (Movie S1). This motility pattern most likely follows microtubular bundles well documented by several ultrastructural studies (6–8, 31).

Dynamic Templates Supported by Actin Meshwork Control Biomineralization. Biomineralization starts within a confined (delineated) space, separated from seawater and associated with the POS (32) located within a distal part of the globopodium (Figs. 2 E and F and 4 *C* and *D*). Formation of the POS (also described as the primary organic membrane) precedes any carbonate mineralization (Fig. 2*C*). Most likely, the POS is formed from secretory activity of the "cytoplasmic envelope" (6), identified as the globopodium at this stage of chamber formation. The POS seems to form a primary nucleation site for the chamber wall (6, 16, 27, 33). Calcification

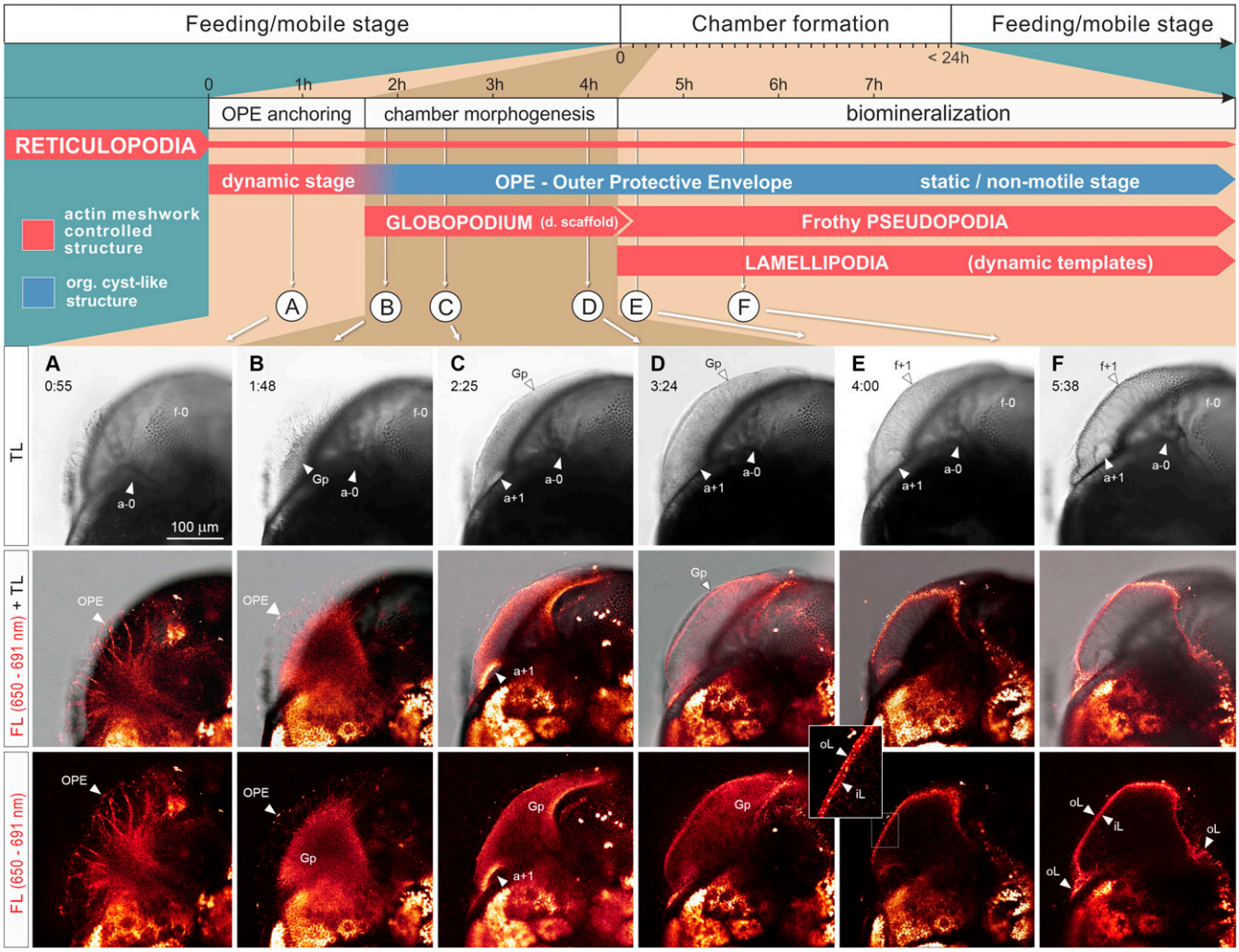

Fig. 2. Successive stages of foraminiferal chamber formation associated with remodeling of actin meshwork. Ventral side of *A. lessonii* shell under transmission and/or fluorescence light under the confocal microscope. Actin stained with SiR-actin is presented in red. Red to bright-yellow microstructures within the existing shell are due to dominating autofluorescence emitted by symbiotic diatoms. All chamber formation stages (*A*–*F*) are strongly dependent on actin meshwork dynamics. (*A*) Formation of OPE with finger-like protuberances attached (anchored) to the substratum. Its dynamic (motile) phase is driven by the actin meshwork. Actin meshwork retreats after formation of the globopodium (Gp) leaving a static (nonmotile) OPE. (*B*) Dynamic growth of Gp with dispersed actin meshwork. (*C*) Shaping of a chamber by expansion of Gp supported by dense radiating rhizopodia, associated with formation of an aperture (a+1). (*D*) Final morphogenetic stage of chamber formation with extension of outer lamellipodium (oL) over the existing shell. (*E*) Internal reorganization of dense radiating rhizopodia to sparsely distributed frothy pseudopopodial structures, followed by onset of chamber (f+1) calcification between the oL and inner lamellipodium (iL). (*Inset*) Magnified oL and iL with a gap between both actin layers, representing the calcifying wall. (*F*) Continuous biomineralization of the chamber (f+1) on internal and external sides of the chamber wall. The secondary calcite layer on top of existing shell is formed under oL associated with actin meshworks. Sparsely distributed frothy pseudopopodia are observed inside f+1 chamber. Aperture (a-0) of final chamber (f-0); aperture (a+1) of constructed chamber (f+1); FL, fluorescent light; Gp, globopodium; TL, transmission light.

continues on both, internal and external, surfaces of the POS. Fig. 2*E* (*Inset*) documents a double-actin meshwork and a thin black gap, representing a thin, partly mineralized, wall in the early stage of $CaCO_3$ biomineralization (Fig. 4 *C* and *D* and Movies S5 and S6). Once biomineralization starts, the globopodial stage ends by definition and the globopodium transforms into two lamellar structures, i.e., an inner and outer lamellipodium, as well as disperses into frothy pseudopodia inside the chamber. The outer lamellipodium coats the outer wall surface during calcification (Fig. 4*D*). The inner lamellipodium is attached to the internal surface of calcified wall and directly connected to the dispersed frothy pseudopodia (Figs. 2 *E* and *F* and 4 *C* and *D*). The term "lamellipodium" is known from various eukaryotic cells (34). Lamellipodia are also recognized in foraminifera and refer to thin (flattened) pseudopodial structures adhered to the substrate, revealing a bidirectional streaming (31).

We assume that lamellipodia create flat compartments that represent the biomineralization site. The active actin meshworks control the structure and distribute molecules, responsible for the nucleation of $CaCO_3$ by attracting Ca^{2+} and carbonate ions. The POS itself, while becoming embedded within the newly calcified wall, can no longer exchange ions with solution (27) neither control further stages of biomineralization (Fig. 4*D*). The biomineralization is subsequently extended over a part or the entire existing shell by the outer lamellipodium (Fig. 2 *E* and *F* and Movie S4). According to Angell (35), this process is initiated when the vesicular cytoplasm leaves the Anlage in the area of the incipient aperture (Fig. 2 *D* and *E*) and forms a sheath around the developing chamber. This active cytoplasmic "sheath" is, in fact, the outer lamellipodium that controls secretion of a calcite layer either over the whole or a part of the existing shell. Erez (32) interpreted this phenomenon as a "self-vacuolization of the

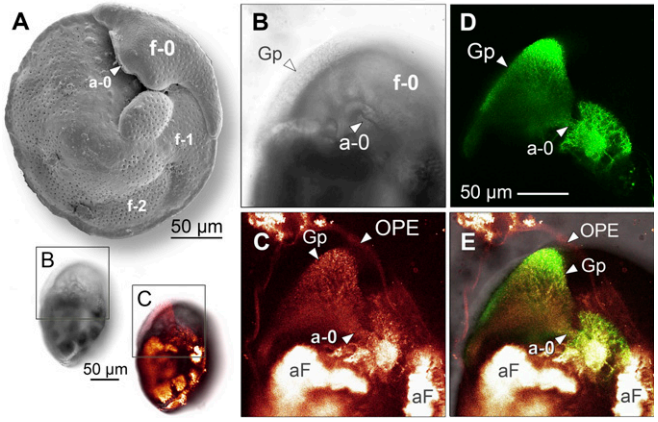

Fig. 3. Benthic foraminifer *A. lessonii* d'Orbigny. Shell growth during initial stage of chamber formation. (*A*) Ventral view of empty shell under SEM. (*B*) Oblique view of ventral side under inverted normal transmission light with close-up of Gp. (*C*) Merged TL and FL with artificial red color expressing emitted light of 650–691 nm representing SiR-actin labeling and strong (orange to white) autofluorescence (aF) of endosymbionts (diatoms); close-up without TL. (*D*) Calcein AM labeling (green) with emission 494–534 nm. (*E*) Merged TL, SiR-actin, and Calcein AM with autofluorescence of symbionts observed within older chambers. Final chamber (f-0) with its aperture (a-0); preceding chambers (f-1 and f-2); aF, autofluorescence.

organisms separating the shell from the environment." This stage was well observed in *A. lessonii* by labeling of the F-actin meshwork within the outer lamellipodium (Fig. 2 *D*–*F* and Movie S4) that enveloped the entire shell at least 3 h after the onset of chamber formation.

Discussion

Dynamic lamellipodia are known from other cells as very active structures responsible for substrate adhesion, cell motility, synaptogenesis, micro/pinocytosis, and phagocytosis (34). In contrast to other eukaryotic cells, where the lamellipodium is usually limited in width from ∼1 to 5 µm (34), the foraminiferal lamellipodium (31) is laterally much more extended, facilitating self-engulfment of the existing relatively large shell (50–2,000 µm). This cellular structure forms a so-called "delimited biomineralization space" (28, 32, 35) over the older chambers or even the whole shell, thereby creating a barrier that seals off the site of calcification from the microenvironment (Fig. 4). It should be stressed that biomineralization in foraminifera does not occur in direct contact with seawater, and therefore, it is not extracellular. This interpretation seems to contradict previous assumptions that biomineralization in nonmiliolid foraminifera is interpreted as extracellular (6, 26, 32, 36). In fact, this is semiintracellular mineralization that resembles "biologically controlled extracellular mineralization" (36), as well as "mineralization of extracellular matrix" models (37). The main point is that the organic matrix (POS) is not extracellular during biomineralization because it is enclosed in active cytoplasmic structures (lamellipodia).

Biomineralization in *A. lessonii*, and most likely in other calcareous globothalamean (rotaliid) foraminifera, cannot occur in direct contact with the cytosol, thus it cannot be strictly intracellular. Calcium ions are known as nearly universal intracellular messengers that have to be kept in a homeostasis at a very low level (38–40). Thus, based on this study, our hypothesis is that biomineralization is limited to a confined space controlled by active cytoplasmic structures. This biomineralization that is separated from the cytosol is therefore called semiintracellular. This interpretation agrees with observations of membrane probes labeling thin ectoplasmic layer that most likely isolated the crystals from the surrounding water during mineralization (32). Recent ultrastructural SEM investigations also document another globothalamean species (*Ammonia*) that revealed isolation of calcification sites by two external organic layers, i.e., inner and outer organic layers, entrapping the POS (41, 42). These external layers, actively involved in calcification

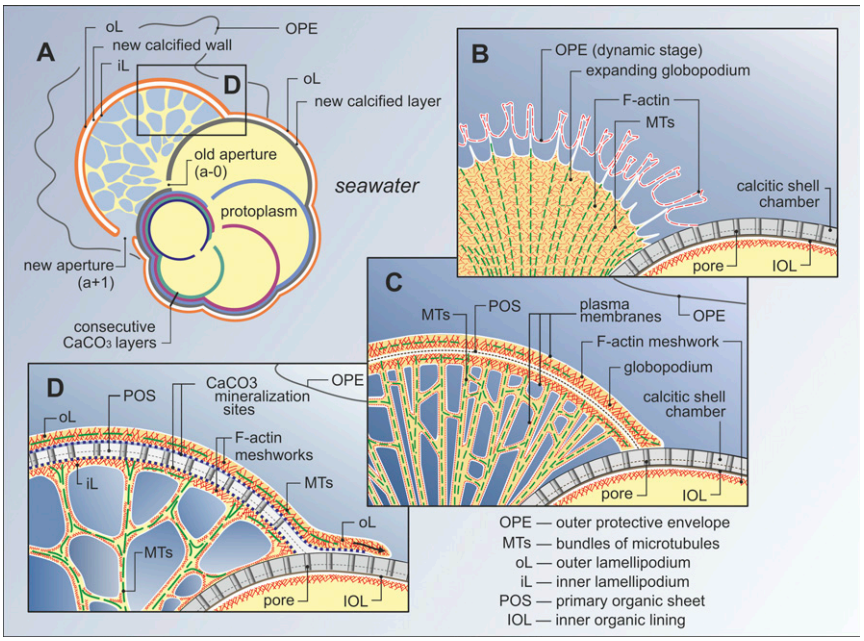

Fig. 4. Emergent model of chamber formation based on observations from live actin staining of calcifying globothalamean foraminifera. Position of microtubules is inferred based on cytoskeleton organization of reticulopodia. (*A*) Cross-section of foraminifer during chamber formation of multilamellar shell with five chambers. It represents the biomineralization stage (*D*) of chamber formation. (*B*) Expanding globopodium from the old aperture, coated by the OPE in its dynamic stage with finger-like protuberances. (*C*) Gp forms the chamber morphology and a POS which is supported by dense radiating rhizopodia; OPE in the passive stage. (*D*) Biomineralization of chamber between oL and iL; engulfment of existing shell by oL; calcification of calcite layer is limited to sites coated by oL; frothy pseudopodia supported by cytoskeletal structures disperse within the internal part of a chamber; cross-sections of elongated compartments probably filled with seawater are presented; OPE in the passive stage.

during the chamber formation, truly represent inner and outer lamellipodial structures identified in *A. lessonii*. Authors suggest an early "leakage" of seawater through tiny holes of outer/inner organic layers at the onset of mineralization (42). Further research is required to investigate this phenomenon and its consequences.

A similar pattern of "calcite layers bounded by inner organic layers formed by the inner and outer cytoplasm" was identified much earlier in planktonic foraminifera (43) that also belong to rotaliid globothalameans (13). Spinose planktonic foraminifera are often coated by a thin and continuous sheath-like structure that forms a cytoplasmic envelope during precipitation of additional calcite layers to the surface of the existing shell (6). This cytoplasmic envelope (i.e., outer cytoplasm) represents the outer lamellipodium described in our study (Figs. 2 *D–F* and 4*D*).

It should be mentioned that sublamellipodial precipitation space observed in rotaliid globothalamean foraminifera differs from precipitation vesicles known from porcelaneous (miliolid) foraminifera (44, 45) that belong to Tubothalamea (13). Such vesicles mineralize bundles of calcite needles randomly deposited within external wall of a constructed chamber (44, 45). Nevertheless, both biomineralization strategies known either from porcelaneous (tubothalamean) or nonporcelaneous (globothalamean) foraminifaera can be assumed as semiintracellular because biomineralization is confined to compartments separated from the cytosol and an external milieu. It should also be emphasized that both mineralization modes produce extracellular shells (tests) enclosing endoplasmic structures.

Biomineralization in globothalamean foraminifera is probably controlled by specific spacing of acidic proteins, which have been identified within the organic matrix of foraminiferal tests before (46–48). The concept of biologically controlled mineralization is based on the "organic matrix-mediated" process actively selecting ions, which induce crystallization and growth (47, 49–51). Such a model for calcification in foraminifera was introduced by Towe and Cifelli (26), who assumed that epitaxial calcification takes place on an active–passive organic matrix.

Based on live staining experiments, we identify dynamic subcellular structures responsible for chamber formation in globothalamean foraminifera. All these structures are dedicated to successive functional stages of chamber formation (Fig. 2). The early (dynamic) stage of the OPE is responsible for anchoring and formation of static organic structure (nonmotile OPE, see Fig. 2). The globopodium acts as a dynamic scaffold responsible for chamber morphogenesis and is followed by development of dynamic lamellipodial templates controlling biomineralization (Figs. 2 and 4). The globopodium molds a chamber morphology and is involved in formation of a POS (Fig. 4).

It should be stressed that all these structures driven by cytoskeletal dynamics precede any calcification activity. $CaCO_3$ nucleation starts from the POS secreted and supported by the globopodial scaffold most likely shaped by the actin meshworks and inferred microtubular structures within radiating rhizopodia (Figs. 2 and 3 *C* and *D*). The overall shape of the chamber is therefore fixed at the end of the globopodial stage (Fig. 2*E* and Movie S5). With the onset of biomineralization, lamellipodia control calcification of a chamber and the simultaneous formation of a layer of $CaCO_3$ on the existing shell. Lamellipodial dynamics differs from the globopodial one because lamellipodia are very flat and evenly attached to a substratum (here the chamber and shell wall). Therefore, the lamellipodium follows the substratum and moves laterally over surfaces without any modification of its overall morphology.

Frothy pseudopodia are most likely responsible for vacuolization (52, 53) and extensive ion exchange between the site of calcification and seawater, such as active outward proton pumping (53, 54). Frothy structures develop at the latest stage of globopodium formation and spread during the biomineralization stage (Figs. 2 and 4). Similar vacuolar structures have been identified based on Calcein AM staining in outer chambers of tubothalamean foraminifera species and interpreted to "play a significant role in seawater transport from the outside of the test" (29). Frothy pseudopodia also resemble peripheral cytoplasm that forms alveolate bubble capsules known from planktonic *Hastigerina pelagica* (d'Orbigny), an extant planktonic foraminifer. Such a single capsule is composed of "closely packed soap bubbles" surrounding the test of *H. pelagica* (6). In contrast to the planktonic species, the frothy pseudopodia in *A. lessonii* are observed mostly inside the constructed chamber during the final stage of the globopodium formation and the following stage of extensive calcification.

All dynamic structures are constructed, as well as driven by dynamic (motile) F-actin meshwork linked to the plasma membranes associated with microtubular structures known from foraminiferal reticulopodia (6–9). Such dynamics is based on continuous reorganization accomplished by assembling and disassembling cytoskeleton proteins in response to changes in external or internal forces (34, 55). A direct association of F-actin meshworks with microtubular structures can be inferred from bidirectional movement of granules that follow relatively straight, linear tracks. Such intracellular motility patterns have been observed in our experiments within all pseudopodial structures, including granuloreticulopodia, globopodium, and lamellipodia, at all stages of chamber formation. The microtubules are known to form a rigid scaffolding within the cytoplasm that provides structural support for elongated strands, as well as setting intracytoplasmic tracks guiding the flow of organelles (6–8, 31). Additional tubulin staining experiments would help identify morphogenetic impact of microtubules and verify the hypotheses that chamber morphology depends on elongation of rhizopodia (1, 14, 17). The overall model of shell formation in foraminifera controlled by the dynamic templates may reveal a universal mechanism for skeleton morphogenesis and semiintracellular biomineralization in unicellular eukaryotes. Biomineralization of single cells therefore occurs in confined spaces represented by compartments controlled by active subcellular structures, driven by actin meshwork dynamics (20–22). Such compartments, including either sublamellipodial delimited spaces (this study) or a variety of deposition vesicles (14–16), appear to be separated from all sides, i.e., cytoplasm and an external microhabitat (e.g., seawater). This semiintracellular biomineralization system produces extracellular mineral skeletons known from various unicellular eukaryotic taxa, including foraminifera, diatoms, and coccolithophores.

Our investigations suggest that dynamics and the spatial organization of scaffolds and templates emerge from the generation of multiscale coordinated forces within pseudopodial structures that behave like the "active gel" (*sensu* ref. 56). Its morphogenetic activity comes from interactions between the membranes and cytoskeleton working in concert with associated proteins and all other building blocks (57, 58). These results partly untangle multiscale complexity of dynamic structures responsible for biologically controlled mineralization, as well as prompt potential applications of dynamic templates in synthetic mineralization of complex architectures controlled by actin meshworks.

Further investigations should focus on other cytoskeleton proteins, such as tubulin, as well as other associated proteins. The most promising approach would be to run actin inhibition experiments, verifying direct impact of F-actin and associated proteins on morphogenesis and biomineralization. Inhibition at various chamber formation stages with variable inhibitor concentrations would test differential impact of actin interactions on organic structures and inorganic components transported to the site of biomineralization. Such experiments should shed light on the vital effect (36, 59) associated with trace element and isotopic variability in foraminiferal shell composition. There is no doubt that future genomic, transcriptomic, and proteomic results will provide further insights into the genetic and epigenetic controls of biomineralization.

Materials and Methods

Living benthic foraminifera were collected from the coral reef aquarium in the Burgers Zoo (60). The samples were transferred to a 10-L aquarium containing seawater with a salinity of 32‰, pH of 8.2, and temperature of 25 °C. Experiments were run on juvenile *A. lessonii* to facilitate observation and staining of several individuals undergoing simultaneous chamber formation events. Live staining was applied to monitor a complete temporal sequence of chamber formation processes. F-actin was labeled with SiR-actin (23). In addition, Calcein AM was used in several double-labeling experiments to stain living cytoplasm via intracellular Ca^{2+} and to compare the overlap with actin cytoskeleton structures. The cell-permeant compound Calcein AM is a nonfluorescent ester which is converted into the green fluorescent calcein when hydrolyzed by intracellular esterases in living cells, including foraminifera (29). All experiments following the same procedures were replicated on several individuals of foraminifera at different chamber formation stages. Staining results were observed and recorded using a Leica SP5 confocal microscope.

Additional information is provided in *SI Appendix, Supplementary Materials and Methods* and Movies S1–S6.

ACKNOWLEDGMENTS. We are grateful to the late L. Hottinger, as well as to S. Abramovich, J. M. Bernhard, J. Erez, C. Hemleben, J. Hohenegger, M. Gutbrod, J. Goleń, N. Keul, G. Langer, Y. Nagai, G. Nehrke, L. de Nooijer, H. Spero, S. Thoms, and T. Toyofuku for encouraging discussions, as well as to N. Höher and G. Rivera-Ingraham for assistance at early experiments, and to B. Müller for technical support. We thank S. S. Bowser and J. L. Travis for expert knowledge of the foraminiferal cytoskeleton and cytoskeletal staining. EU FP7 Project 285989 (to J.T., M.R., and J.B.), the Kosciuszko Foundation Grant (to J.T.), and the Grzybowski Foundation travel grant (to J.T.) are acknowledged. This research was supported by the Polish National Science Center (Grant DEC-2015/19/B/ST10/01944 to J.T.) and by the German Research Foundation (DFG) through Research Grant RA 2068/3-1 (to M.R.) and a joint ANR-DFG Project Grant BI 432/10-1 (to J.B). The authors acknowledge Scientific Committee on Oceanic Research WG 138 support.

1. Hottinger L (1986) Construction, structure, and function of foraminiferal shells. *Biomineralization in Lower Plants and Animals*, eds Leadbeater BSC, Riding R (Clarendon, Oxford), Vol 30, pp 219–235.
2. Monteiro FM, et al. (2016) Why marine phytoplankton calcify. *Sci Adv* 2:e1501822.
3. Thomson DW (1917) *On Growth and Form* (Cambridge Univ Press, Cambridge, UK), pp 1–793.
4. Goodwin BC (1989) Unicellular morphogenesis. *Cell Shape: Determinants, Regulation, and Regulatory Role*, eds Stein WD, Bronner F (Academic, San Diego), pp 365–391.
5. Ingber DE (1993) Cellular tensegrity: Defining new rules of biological design that govern the cytoskeleton. *J Cell Sci* 104:613–627.
6. Schiebel R, Hemleben C (2017) *Planktic Foraminifers in the Modern Ocean* (Springer, Berlin), pp 1–358.
7. Bowser SS, Travis JL, Rieder CL (1988) Microtubules associate with actin-containing filaments at discrete sites along the ventral surface of *Allogromia* reticulopods. *J Cell Sci* 89:297–307.
8. Travis JL, Bowser SS (1986) Microtubule-dependent reticulopodial motility: Is there a role for actin? *Cell Motil Cytoskeleton* 6:146–152.
9. Travis JL, Bowser SS (1991) The motility of Foraminifera. *Biology of Foraminifera*, eds Lee JJ, Anderson OR (Academic, New York), pp 91–155.
10. Lipps JH (1993) *Fossil Prokaryotes and Protists* (Blackwell, Cambridge, MA), pp 1–352.
11. Langer MR (2008) Assessing the contribution of foraminiferan protists to global ocean carbonate production. *J Eukaryot Microbiol* 55:163–169.
12. Knoll AH, Kotrc B (2015) Protistan skeletons: A geologic history of evolution and constraint. *Evolution of Lightweight Structures*, ed Hamm C (Springer, Dordrecht, The Netherlands), pp 1–16.
13. Pawlowski J, Holzmann M, Tyszka J (2013) New supraordinal classification of Foraminifera: Molecules meet morphology. *Mar Micropaleontol* 100:1–10.
14. Tyszka J (2006) Morphospace of foraminiferal shells: Results from the moving reference model. *Lathaia* 39:1–12.
15. Hemleben C (1969) Zur morphogenese planktonischer Foraminiferen. *Zitteliana* 1:91–133.
16. Hemleben C, Spindler M, Anderson OR (1989) *Modern Planktonic Foraminifera* (Springer, New York).
17. Tyszka J, Topa P, Saczka K (2005) State-of-the-art in modelling of foraminiferal shells: Searching for an emergent model. *Stud Geol Pol* 124:143–157.
18. Topa P, Tyszka J, Bowser SS, Travis JL (2012) DPD model of foraminiferal chamber formation: Simulation of actin meshwork—Plasma membrane interactions. *Lect Notes Comput Sci* 7204:588–597.
19. van de Meene AML, Pickett-Heaps JD (2002) Valve morphogenesis in the centric diatom *Proboscia alata* Sundstrom. *J Phycol* 38:351–363.
20. Tesson B, Hildebrand M (2010) Dynamics of silica cell wall morphogenesis in the diatom *Cyclotella cryptica*: Substructure formation and the role of microfilaments. *J Struct Biol* 169:62–74.
21. Langer G, De Nooijer LJ, Oetjen K (2010) On the role of the cytoskeleton in coccolith morphogenesis: The effect of cytoskeleton inhibitors. *J Phycol* 46:1252–1256.
22. Durak GM, Brownlee C, Wheeler GL (2017) The role of the cytoskeleton in biomineralisation in haptophyte algae. *Sci Rep* 7:15409.
23. Lukinavičius G, et al. (2014) Fluorogenic probes for live-cell imaging of the cytoskeleton. *Nat Methods* 11:731–733.
24. Reiss Z (1957) The Bilamellidea, nov. superfam., and remarks on Cretaceous globorotaliids. *Contrib Cushman Found Foram Res* 8:127–145.
25. Angell RW (1967) The process of chamber formation in the foraminifer *Rosalina floridana* (Cushman). *J Protozool* 14:566–574.
26. Towe KM, Cifelli R (1967) Wall ultrastructure in the calcareous foraminifera: Crystallographic aspects and a model for calcification. *J Paleontol* 41:742–762.
27. Branson O, et al. (2016) Nanometer-scale chemistry of a calcite biomineralization template: Implications for skeletal composition and nucleation. *Proc Natl Acad Sci USA* 113:12934–12939.
28. Bé AWH, Hemleben C, Anderson OR, Spindler M (1979) Chamber formation in planktonic foraminifera. *Micropaleontology* 25:294–306.
29. Ohno Y, Fujita K, Toyofuku T, Nakamaura T (2016) Cytological observations of the large symbiotic foraminifer *Amphisorus kudakajimensis* using calcein acetoxymethyl ester. *PLoS One* 11:e0165844.
30. Bernhard JM, Blanks JK, Hintz CJ, Chandler TG (2004) Use of the fluorescent calcite marker calcein to label foraminifera tests. *J Foraminiferal Res* 34:96–101.
31. Travis JL, Kenealy JF, Allen RD (1983) Studies on the motility of the foraminifera. II. The dynamic microtubular cytoskeleton of the reticulopodial network of *Allogromia laticollaris*. *J Cell Biol* 97:1668–1676.
32. Erez J (2003) The source of ions for biomineralization in foraminifera and their implications for paleoceanographic proxies. *Rev Mineral Geochem* 54:115–149.
33. Spero HJ (1988) Ultrastructural examination of chamber morphogenesis. *Mar Biol* 99:9–20.
34. Small JV, Stradal T, Vignal E, Rottner K (2002) The lamellipodium: Where motility begins. *Trends Cell Biol* 12:112–120.
35. Angell RW (1979) Calcification during chamber development in *Rosalina floridana*. *J Foraminiferal Res* 9:341–353.
36. Weiner S, Dove PM (2003) An overview of biomineralization processes. *Rev Mineral Geochem* 54:1–29.
37. Weiner S, Addadi L (2011) Crystallization pathways in biomineralization. *Annu Rev Mater Res* 41:21–40.
38. Schanne FA, Kane AB, Young EE, Farber JL (1979) Calcium dependence of toxic cell death: A final common pathway. *Science* 206:700–702.
39. Rasmussen H, Barrett P, Smallwood J, Bollag W, Isales C (1990) Calcium ion as intracellular messenger and cellular toxin. *Environ Health Perspect* 84:17–25.
40. Schenck PA, Chew DJ, Nagode LA, Rosol TJ (2009) Disorders of calcium: Hypercalcemia and hypocalcemia. *Current Diagnosis and Treatment Nephrology and Hypertension*, eds Berns JS, Lerma E, Nissenson AR (McGraw-Hill, New York), pp 122–194.
41. Nagai Y, Uematsu K, Wani R, Toyofuku T (2018) Reading the fine print: Ultra-microstructures of foraminiferal calcification revealed using focused ion beam microscopy. *Front Mar Sci* 5: 67.
42. Nagai Y, et al. (2018) Weaving of biomineralization framework in rotaliid foraminifera: Implications for paleoenvironmental reconstructions. *Biogeosciences* 15: 6773–6789.
43. Hemleben C, Be AWH, Anderson OR, Tuntivate S (1977) Test morphology, organic layers and chamber formation of the planktonic foraminifer *Globorotalia menardii* (d'Orbigny). *J Foraminiferal Res* 7:1–25.
44. Berthold W-U (1976) Biomineralisation bei milioliden foraminiferen und die Matritzen-hypothese. *Naturwissenschaften* 63:196–197.
45. Hemleben C, Anderson OR, Berthold W (1986) Calcification and chamber formation in Foraminifera–Brief overview. *Biomineralization in Lower Plants and Animals*, eds Leadbeater BSC, Riding R (Clarendon Press, Oxford), Vol 30, pp 237–249.
46. Weiner S, Erez J (1984) Organic matrix of the shell of the foraminifer, *Heterostegina depressa*. *J Foraminiferal Res* 14:206–212.
47. Weiner S, Addadi L (1997) Design strategies in mineralized biological materials. *J Mater Chem* 7:689–702.
48. Langer MR (1992) Biosynthesis of glycosaminoglycans in foraminifera: A review. *Mar Micropaleontol* 19:245–255.
49. Robbins LL, Brew K (1990) Proteins from the organic matrix of core-top and fossil planktonic foraminifera. *Geochim Cosmochim Acta* 54:2285–2292.
50. Addadi L, Weiner S (1985) Interactions between acidic proteins and crystals: Stereochemical requirements in biomineralization. *Proc Natl Acad Sci USA* 82:4110–4114.
51. Lowenstam HA (1981) Minerals formed by organisms. *Science* 211:1126–1131.
52. Bentov S, Brownlee C, Erez J (2009) The role of seawater endocytosis in the biomineralization process in calcareous foraminifera. *Proc Natl Acad Sci USA* 106:21500–21504.
53. de Nooijer LJ, Spero HJ, Erez J, Bijma J, Reichart GJ (2014) Biomineralization in perforate foraminifera. *Earth Sci Rev* 135:48–58.
54. Toyofuku T, et al. (2017) Proton pumping accompanies calcification in foraminifera. *Nat Commun* 8:14145.
55. Pollard TD, Borisy GG (2003) Cellular motility driven by assembly and disassembly of actin filaments. *Cell* 112:453–465.
56. Prost J, Jülicher F, Joanny JF (2015) Active gel physics. *Nat Phys* 11:111–117.
57. Pouget E, et al. (2007) Hierarchical architectures by synergy between dynamical template self-assembly and biomineralization. *Nat Mater* 6:434–439.
58. Fletcher DA, Mullins RD (2010) Cell mechanics and the cytoskeleton. *Nature* 463: 485–492.
59. Nehrke G, Keul N, Langer G, De Nooijer LJ, Bijma J (2013) A new model for biomineralization and trace-element signatures of Foraminifera tests. *Biogeosciences* 10:6759–6767.
60. Ernst S, et al. (2011) Benthic foraminifera in a large Indo-Pacific coral reef aquarium. *J Foraminiferal Res* 41:101–113.